DSMC and Navier–Stokes Study of Backflow for Nozzle Plumes Expanding into Vacuum

P.V. Vashchenkov, A.N. Kudryavtsev, D.V. Khotyanovsky, M.S. Ivanov

Institute of Theoretical and Applied Mechanics, 4/1, ul. Institutskaya, Novosibirsk 630090, Russia

Abstract. An important problem for space vehicles is contamination of the spacecraft surface by combustion products and unburned fuel exhausting from control thruster nozzles. The objective of the present work is a detailed simulation of the backflow in the case of gas exhaustion from the nozzle into vacuum. A specific feature of this problem is the drastic expansion of the initially dense flow at the nozzle exit, which makes necessary simulations of the near-continuum flow inside the nozzle, the transitional flow near the nozzle exit, and the free-molecular flow outside the nozzle. The simulations are performed by a combined Navier-Stokes/DSMC approach.

INTRODUCTION

An important problem arising in long-term operation of space vehicles is contamination of the spacecraft surfaces with the combustion products issuing from the nozzles of the control thrusters (see ref. [1]). During thruster firing, a large amount of propellant is exhausted into space, and droplets forming as a result of liquid fuel condensation and breakup of the nozzle cooling film can reach the spacecraft surface. One of the possible mechanisms provoking the reverse motion of liquid droplets may be the carrier-gas backflow originating from the nozzle boundary layer, which turns sharply around the nozzle lip while undergoing continuum expansion and then passing into transitional and free-molecular regimes as the density decreases. It can be assumed that the gas flow drags the droplets from the nozzle into the backflow region.

In this paper we simulate the gas flow exhausting from a supersonic nozzle with Reynolds number Re = 590. In addition, we performed a study of the mechanisms of the flow turn around the nozzle lip and the backflow origination. A specific feature of this problem is the drastic expansion of the initially dense flow, which makes necessary using the combined Navier–Stokes/DSMC approach.

NUMERICAL APPROACH

The two-dimensional and axisymmetric Navier-Stokes equations are solved with a shock-capturing MUSCL TVD scheme. The standard van Leer's formula with the *minmod* slope limiter [2] is used for reconstruction of cell-faced variables from cell-centered ones. The viscous terms are approximated by the central finite differences. The HLLEM approximate Riemann solver [3] is employed to calculate the inviscid fluxes. The HLLEM solver is constructed to be robust near low densities and, therefore, it is particularly appropriate for simulation of rapidly expanding flows such as in the present paper.

For low-Reynolds-number regimes, the initial rarefaction effects are taken into account by means of imposing velocity slip and temperature jump boundary conditions on solid walls. For this purpose, the slip conditions deduced by Kogan [4] are used.

The DSMC code SMILE [5] developed in Computational Aerodynamics Laboratory, Institute of Theoretical and Applied Mechanics is utilized for kinetic modeling. Intermolecular collisions are computed by the Variable Hard Sphere (VHS) model. The number of collisions is calculated by the majorant frequency method. In the case of a polyatomic gas, the energy redistribution between rotational and translational degrees of freedom is obtained in accordance with the Larsen-Borgnakke model [6] with a constant rotational collision number. Up to $9.6 \cdot 10^6$ molecules are used to simulate the flows under consideration. The computations are performed on a 32-processor Linux cluster.

		Form Approved OMB No. 0704-0188

Report Documentation Page

1. REPORT DATE **13 JUL 2005**	2. REPORT TYPE **N/A**	3. DATES COVERED **-**
4. TITLE AND SUBTITLE **DSMC and NavierStokes Study of Backflow for Nozzle Plumes Expanding into Vacuum**		5a. CONTRACT NUMBER
		5b. GRANT NUMBER
		5c. PROGRAM ELEMENT NUMBER
6. AUTHOR(S)		5d. PROJECT NUMBER
		5e. TASK NUMBER
		5f. WORK UNIT NUMBER
7. PERFORMING ORGANIZATION NAME(S) AND ADDRESS(ES) **Institute of Theoretical and Applied Mechanics, 4/1, ul. Institutskaya, Novosibirsk 630090, Russia**		8. PERFORMING ORGANIZATION REPORT NUMBER
9. SPONSORING/MONITORING AGENCY NAME(S) AND ADDRESS(ES)		10. SPONSOR/MONITOR'S ACRONYM(S)
		11. SPONSOR/MONITOR'S REPORT NUMBER(S)
12. DISTRIBUTION/AVAILABILITY STATEMENT **Approved for public release, distribution unlimited**		
13. SUPPLEMENTARY NOTES **See also ADM001792, International Symposium on Rarefied Gas Dynamics (24th) Held in Monopoli (Bari), Italy on 10-16 July 2004. , The original document contains color images.**		
14. ABSTRACT		
15. SUBJECT TERMS		

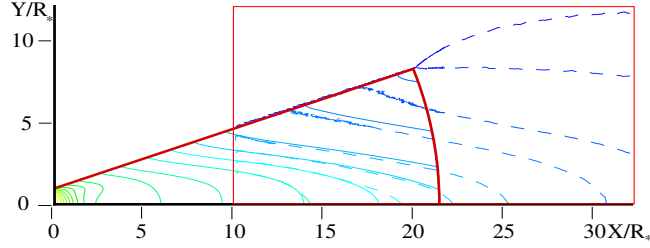| 16. SECURITY CLASSIFICATION OF:			17. LIMITATION OF ABSTRACT **UU**	18. NUMBER OF PAGES **6**	19a. NAME OF RESPONSIBLE PERSON
a. REPORT **unclassified**	b. ABSTRACT **unclassified**	c. THIS PAGE **unclassified**			

FIGURE 1. An example of the hybrid continuum/kinetic simulation of low-Reynolds-number flow in a conical nozzle.

In the course of hybrid simulations, a coupling of Navier-Stokes solver and the DSMC method is based on the use of the NS solver in the nozzle and in the plume core and the DSMC method in the neighborhood of the nozzle lip and in the backflow region. Flow parameters on the boundaries of the DSMC computational domain, which are located inside the nozzle and in the central part of nozzle plume, are taken from a previous Navier-Stokes simulation. The velocity distribution function, which is needed to provide necessary boundary conditions for the DSMC method, is specified as the local Maxwellian distribution. It is worth noting that, from the general viewpoint, the Chapman-Enskog distribution function is a natural choice for model particles coming into the DSMC computational domain at the boundary between the NS and DSMC domains. However, the Chapman-Enskog distribution function has a drawback: it becomes negative with deviation from the Maxwellian distribution. Moreover, it was demonstrated in a number of works (see, e.g. [7]) that the Chapman-Enskog distribution function may not provide much improvements against the Maxwellian distribution.

RESULTS

Gas exhausting from nozzle was modelled on the first stage of computations. The nozzle geometry and flow parameters were taken from Rothe's experiments [8]. Corresponding nozzle and flow parameters are: throat radius $R_* = 2.55$ mm, exit radius $R_e = 20.92$ mm, stagnation temperature $T_0 = 300$ K, stagnation pressure $p_0 = 945$ Pa, Reynolds number Re = 590. The density flowfields computed in this case with the Navier–Stokes solver inside the nozzle and by the DSMC method for the external flow are shown in Fig. 1. The domains of the computations made by these two methods overlap in some region near the nozzle exit. The boundaries of computational domains are shown with red lines. The density contours are shown as solid (for Navier-Stokes) and dashed (for DSMC) curves. From this figure, close agreement between two solutions in the common part of two computational domains is evident.

The density distribution along the nozzle axis and the density distribution across the nozzle close to the nozzle exit are shown in Fig. 2. Here the results of the Navier–Stokes simulations (with slip and no-slip conditions on the wall) and the DSMC results are compared with the experimental data obtained in Rothe's experiments. The numerical results along the axis compare well with the experiment along the whole nozzle length. However, as is seen in Fig. 2, the flow near the nozzle axis is poorly reproduced in Navier–Stokes computations with the no-slip conditions. The slip conditions yield results which are closer to the experiment.

In addition, we investigated the flow around the nozzle lip for three nozzle lip shapes: sharp lip, and two rounded lips with the radii $1.67 \cdot 10^{-4}$ m and $6.11 \cdot 10^{-4}$ m. The DSMC simulations were performed in a small domain near the nozzle lip. The inflow data were input into the DSMC simulations from the results of the Navier–Stokes computations.

Figure 3 shows the mass flux isolines for three different nozzle lip shapes. Integral mass flow rate in the reverse direction normalized on total mass flow rate through the nozzle was $1.46 \cdot 10^{-3}$ for the nozzle with a sharp lip, $1.33 \cdot 10^{-3}$ – for the nozzle lip rounded with the radius $1.67 \cdot 10^{-4}$ m, and $9.91 \cdot 10^{-4}$ – for the nozzle lip rounded with the radius $6.11 \cdot 10^{-4}$ m. It is therefore evident that the higher is the rounding radius of the nozzle lip the lower is the backflow component of the mass flow rate from the nozzle.

To further investigate the origin of the backflow we performed additional computations of the flow exhausting from the nozzle. Outside the nozzle, in the backflow region, we set up a screen located at some height above the outer contour of the nozzle (see Fig. 4). The purpose of this screen was to separate different backflow components: let the backflow originated near the nozzle wall go through, but eliminate possible backflow from the periphery of the nozzle plume.
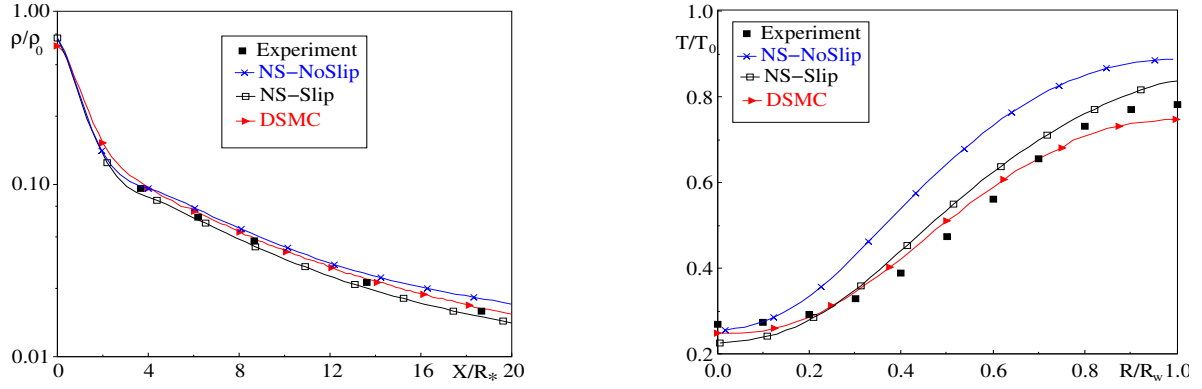
FIGURE 2. Density distribution along the nozzle axis (left) and across the nozzle at $X/R^* = 18.7$ (right)
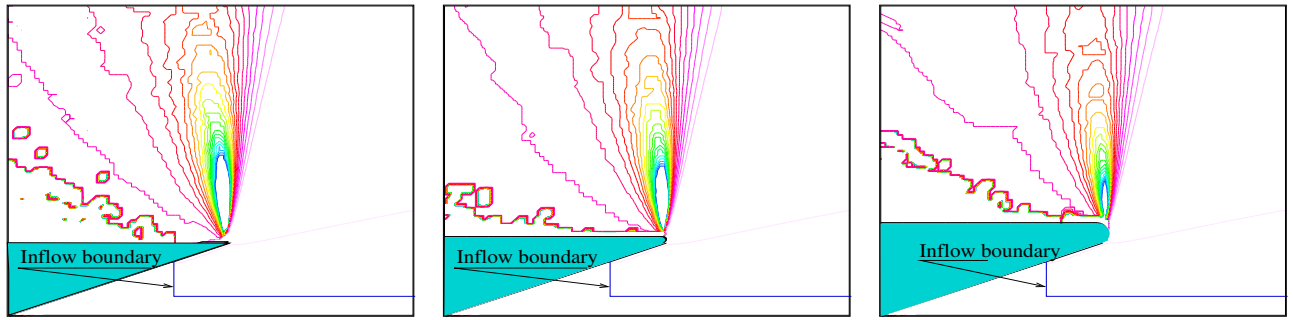

FIGURE 3. Mass flux fields for three different shapes of the nozzle lip

Figure 4 presents density isolines in the backflow region obtained with and without the screen. As seen in the figure, the density flowfield is changed at some distance from the outer contour of the nozzle and is unchanged near the outer nozzle wall. The density and mass flux distributions in radial direction behind the screen are shown in Fig 5. Is is clear that the screen The presence of the screen leads to a very significant decrease in density on the left side of the screen. It means that the most part of the backflow gas comes from the plume rather than from the nozzle boundary layer. It can be assumed that the mechanism of backflow origination from the plume is purely kinetic — molecules on the plume periphery gain an oppositely directed velocity owing to intermolecular collisions.
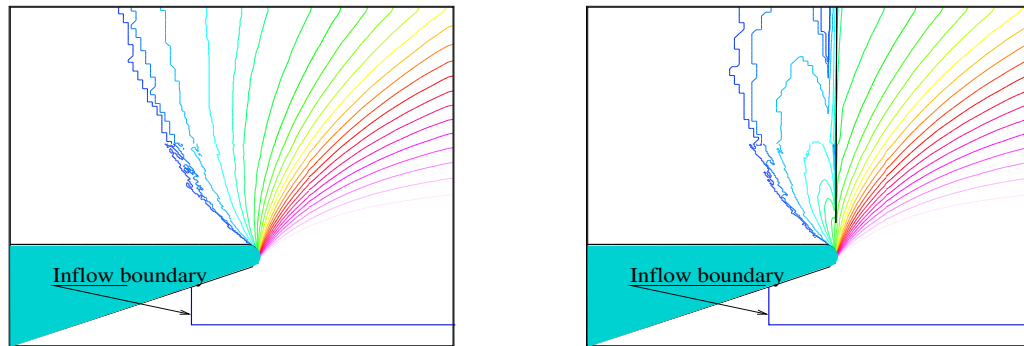

FIGURE 4. Backflow formation on the lip: without screen (left) and with screen (right)
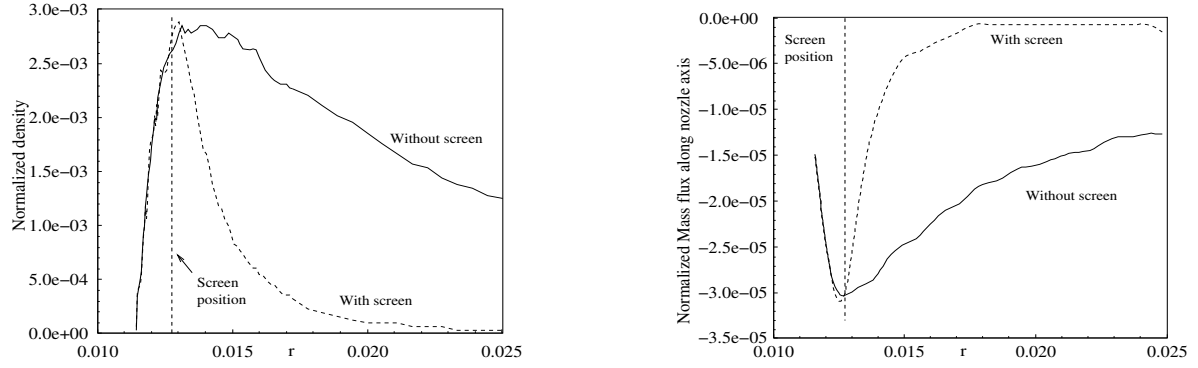
FIGURE 5. Radial distribution of density (left) and mass flux (right) behind the screen

VISCOUS FLOW AROUND AN EXPANSION CORNER

Based on the results described above, it is evident that the investigation of flow expansion around the nozzle lip is critically important for studying backflow contamination. For an inviscid flow, it is well known from the Prandtl–Meyer solution that there is a limiting flow deflection angle. At this limiting angle, all internal energy of the gas transforms into kinetic energy of motion, so that the flow temperature becomes zero while the Mach number keeps growing up to infinity. The viscosity effects can change the expansion flow substantially and, in particular, they favor flow turning by large angles and backflow formation. To investigate this phenomenon in more detail, we consider here a model problem consisting of the two-dimensional flow over an expansion corner formed by a plane wall (flat plate) suddenly deflecting by a large angle. The wall deflection angle φ_w is varied in different simulations. To exclude any influence of models governing the exchange between translational and internal degrees of freedom of molecules, a monatomic gas ($\gamma = 5/3$, Argon) is considered. The simulations were performed with inviscid conditions (non-permeability for Navier-Stokes simulations, specular reflection for DSMC). The simulations were performed for the following flow parameters: the inflow Mach number $M_\infty = 4.38$ and static flow temperature $T_\infty = 75$ K. The unit Reynolds number was varied Re $= 476, 4760, 47600$ to investigate the effects of flow viscosity. The flow was simulated by the DSMC method and with the Navier–Stokes equations. The Navier–Stokes computations were performed for the expansion corner of $\varphi_w = 37.1°$, which coincides with the maximum Prandtl–Meyer angle $\varphi_{\max}$ for $\gamma = 5/3$ and $M_\infty = 4.38$. Note, the maximum Prandtl–Meyer angle for $\gamma = 5/3$ and $M_\infty = 1$ is $90°$. The DSMC computations were performed with $\varphi_w = 37.1°$ and also with $\varphi_w = 180°$, the latter simulates expansion into vacuum around the nozzle lip. The flow was assumed to be two-dimensional.

The typical flowfields obtained are shown in Fig. 6. These computations were performed at the Reynolds number Re $= 47600$, the wall defelection angle in the DSMC simulation was $\varphi_w = 180°$. A close resemblance of two flowfields is worth noting, it holds in spite of the different shape of the computational domains used. Further, it is evident from the flowfields that the numerical solutions are close to the classical Prandtl–Meyer solution only in some range of polar angles φ (here $\varphi = 0$ corresponds to the axis going along Wall 1, and φ is positive in the clockwise direction). Another interesting feature of the solutions obtained is a non-monotonous behavior of the Mach number: starting from some φ it begins to increase.

The angular distributions of the flow parameters (non-dimensional density ρ/ρ_∞, Mach number, temperature T/T_∞ and the flow velocity normalized on maximum adiabatic velocity $|\vec{u}|/u_m$) are given in Figs. 7 and 8. These distributions were recorded along the circle with radius $r/L = 0.4$ centered at the vertex of the expansion corner. For comparison, the inviscid Prandtl–Meyer analytical solution is also plotted in the figures. The DSMC computations in this case were performed for wall deflection $\varphi_w = \varphi_{\max} = 37.1°$ and also for flow expansion into vacuum around the trailing edge, i.e. for wall deflection $\varphi_w = 180°$. These results are very close to each other, hence only $\varphi_w = \varphi_{\max} = 37.1°$ data are given in the figures.

It is evident that the flow viscosity substantially changes the flow around the corner even if the inviscid wall boundary conditions are imposed. This is manifested in termination of growth of the flow Mach number at some polar angle, whose value depends on the Reynolds number, and also in an excessive increase in flow temperature compared to the Prandtl–Meyer solution. These changes become more apparent as the flow Reynolds number decreases. Note, the flow parameters tend to their inviscid limit with increasing Reynolds number. It should be noted that $\varphi_{\max}$ is based on the
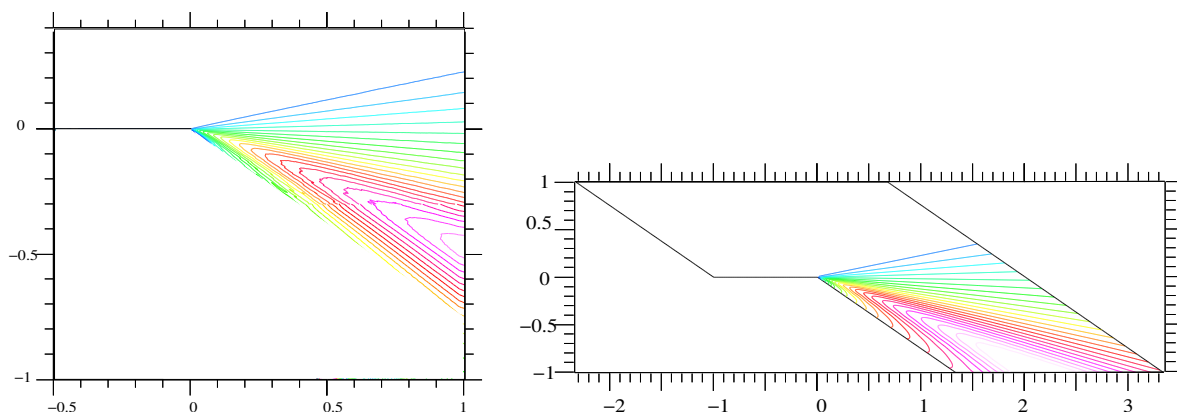
FIGURE 6. Mach flowfields computed by the DSMC method (upper) and by the Navier-Stokes solver (lower)
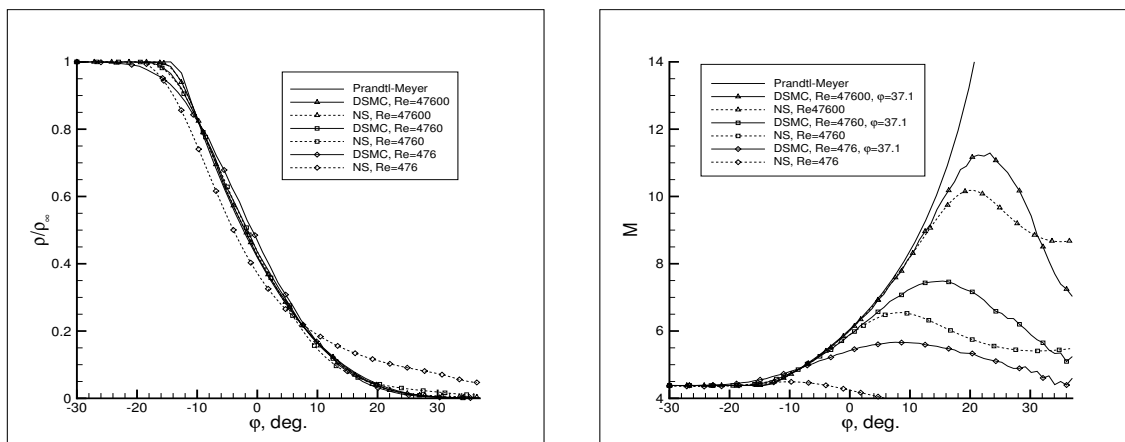

FIGURE 7. Angular distribution of density (left) and Mach number (right) around the expansion corner
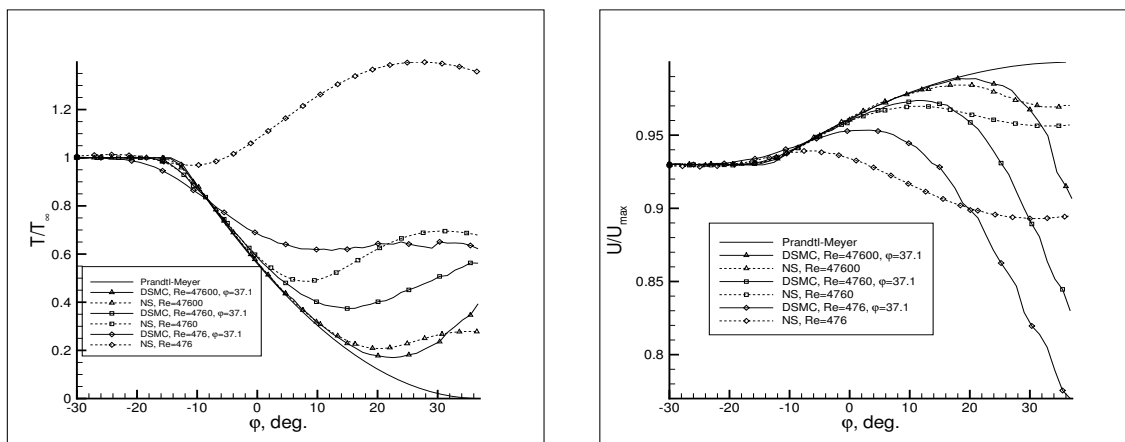

FIGURE 8. Angular distribution of temperature (left) and velocity (right) around the expansion corner

inviscid theory and does not necessarily hold in this case where the viscous forces produce their effects. Still, in the absence of the boundary layers on the walls that form the expansion corner, the inviscid theory predicts the maximum turning angle quite well. Nevertheless, the density in the Navier–Stokes computations performed with Re = 476 is quite different from zero even for $\varphi = \varphi_{\max}$. The latter, Re = 476, case demonstrates the most prominent differences of the Navier–Stokes results compared to the DSMC computations. These differences are evident in this case from the very beginning of flow expansion. The flow Mach number in Navier–Stokes computations does not grow at all. This is caused by the growth of flow temperature due to the work of viscous forces. Based on this, we can conclude that the Navier–Stokes equations are not applicable to simulation of flow expansion at such a low Reynolds number. For higher Reynolds numbers, i.e., for Re = 4760 and Re = 47600, the Navier–Stokes results are in close agreement with the DSMC computations up to the polar angles $\varphi \approx 5°$ and $\varphi \approx 15°$, respectively.

We can conclude that the use of the combined Navier–Stokes/DSMC approach for simulation of the flow around the nozzle lip is essentially important since the Navier–Stokes approach become no longer acceptable as the flow is expanded.

CONCLUSIONS

A detailed numerical investigation of the backflow formation phenomenon for nozzle plumes expanding into vacuum has been performed by a hybrid approach combining the continuum (Navier-Stokes) and kinetic (DSMC) computations.

The flow around the nozzle lip has been investigated in detail for different shapes of the nozzle lip (sharp and rounded). It has been found that the mass flow rate in the backflow region is rather small, amounting approximately to 10^{-3} of the total mass flux through the nozzle. The simulation also demonstrate that intermolecular collisions in the plume peripheral zone contribute substantially to formation of the low-density backflow.

The viscous expansion flow over an expansion corner has been investigated to elucidate details of backflow formation near the nozzle lip. The results of Navier–Stokes and DSMC simulation have been compared and analyzed. It has been found that the effects of viscosity become more significant with the flow expansion and dominate in the rarefied regime. The influence of viscous dissipation causes a decrease in the Mach number and a growth of temperature in contrast with the inviscid Prandtl–Meyer solution.

ACKNOWLEDGMENTS

REFERENCES

1. Hastings, D. and Garrett, H., *Spacecraft-Environment Interactions*, Cambridge Univ. Press., Cambridge, UK, 1996.
2. Yee, H.C., "A Class of High-Resolution Explicit and Implicit Shock-Capturing Methods", *NASA Technical Memorandum 101088*, 1989.
3. Einfeldt, B., Munz, C.D., Roe, P.L., and Sjögreen, B. "On Godunov-Type Methods Near Low Densities", *Journal of Computational Physics*, Vol. 92, No. 2, 1991, pp. 273–295.
4. Kogan, M.N., *Rarefied Gas Dynamics*, Plenum Press, New York, 1969.
5. Ivanov, M.S., Markelov, G.N., Gimelshein, S.F. "Statistical Simulation of Reactive Rarefied Flows: Numerical Approach and Applications", *AIAA Paper 98-2669*, 1998.
6. Borgnakke, C. and Larsen, P.S., "Statistical Collision Model for Monte Carlo Simulation of Polyatomic Gas Mixture", *Journal of Computational Physics*, Vol. 18, No. 3, 1975, pp. 405–420.
7. Wadsworth, D.C., Erwin, D.A., "Two-dimensional Hybrid Continuum/Particle Approach for Rarefied Flows", *AIAA Paper 92-2975*, 1992.
8. Rothe, D., "Electron-Beam Studies of Viscous Flow in Supersonic Nozzles", *AIAA Journal*, Vol. 9, No. 5, 1971, pp. 804–811.